doi:10.3772/j.issn.1006-6748.2024.02.007

Research on static characteristic of double redundance double nozzle flapper valve based on AMESim①

SUN Yanan* (孙亚南), LIANG Qiuhui**, WANG Wentao*, YANG Guang*, ZHANG Wei②**
(* Shijiazhuang Haishan Industrial Development Co. Ltd, Shijiazhuang 050200, P. R. China).
(** Fluid Power Transmission and Control Laboratory, Yanshan University, Qinhuangdao 066004, P. R. China)

Abstract

The feedback spring rod of the armature assembly is cancelled in the double redundance double nozzle flapper valve (DRDNFV), and the difficulty of valve core displacement control is increased. Therefore, this paper intends to study the static characteristic of DRDNFV through the AMESet and AMESim simulation. It is explored under the circumstance of the fixed orifices being clogged and experimentally verified on the test bench. The results show that the pressure gain increases and the flow gain decreases with the increasing clogged degree of the fixed orifices on both sides. The zero bias increases synchronously with the increasing clogged degree of the unilateral fixed orifice. The experimental results are basically consistent with the theoretical curves and the theoretical correctness of the simulation model is effectively verified. The results can provide the theoretical reference for design, debugging, maintenance and fault diagnosis of DRDNFV.

Key words: double redundance double nozzle flapper valve (DRDNFV), AMESet, torque motor, armature assembly, fault diagnosis

0 Introduction

The double nozzle flapper electro-hydraulic servo valve can convert the tiny electrical signal into large power hydraulic signal, which has fast dynamic response, high control precision and long service life. Therefore, it is widely used in the electro-hydraulic servo control system in aviation, aerospace, chemical industry and other fields[1].

In recent years, many scholars have carried out various simulation modeling research on the double nozzle flapper electro-hydraulic servo valve, and achieved the fruitful results. Chen et al.[2] obtained the static and dynamic equations of the single-stage double nozzle flapper electro-hydraulic servo valve by mathematical modeling. It was concluded that the static output pressure and flow were linearly proportional to the input current. Chen[3] studied the pressure characteristic of single-stage nozzle flapper electro-hydraulic servo valve and analyzed the influence of different working conditions on the dynamic and static characteristics of the valve. Wang et al.[4] explained the process of sub-model modeling of armature assembly self-defined with AMESet in detail and established the simulation model of double nozzle flapper electro-hydraulic servo valve. The correctness of the model was verified by the simulation curves. Li[5] established a multidisciplinary physical model of the double nozzle flapper electro-hydraulic servo valve based on the Simcape modeling toolbox in Simulink. The model did not involve complex mathematical formulas and had high precision. Gordic et al.[6] established a simulation model of electro-hydraulic servo valve in Simulink and analyzed the influence of some factors of the valve on its performance. Zhang[7] built the AMESim simulation model of double nozzle flapper electro-hydraulic servo valve, and carried out the fault diagnosis. The particle swarm optimization-conjugate gradient-backpropagation (PSO-CG-BP) neural network model was proposed, and the accuracy, reliability and scientific nature of the model were verified, which was used in the field of fault diagnosis of the servo valve.

Compared with the conventional double nozzle flapper electro-hydraulic servo valve, the valve studied in this paper includes two sets of torque motor, armature, and nozzle flapper assemblies. The feedback spring rod is replaced by the displacement sensor —— linear variable differential transformer (LVDT) at the right end to transmit the feedback signal to form closed-

① Supported by the National Natural Science Foundation of China (52075468), the General Project of Natural Science Foundation of Hebei Province (E2020203052), the Open Fund Project of Shaanxi Provincial Key Laboratory of Hydraulic Technology (YYJS2022KF14) and the Basic Innovation Research Cultivation Project of Yanshan University (2021LGZD003).

② To whom correspondence should be addressed. E-mail: zhangwei@ysu.edu.cn.

Received on May 12, 2023

loop control. The complexity and control difficulty of the valve are increased. The small fixed orifice is clogged easily[8], and it may cause serious failure of the valve and affect the operation stability and reliability.

Therefore, the armature assembly model is established through AMESet and the whole AMESim simulation model of the valve is established in this paper. The pressure and flow characteristics curves are obtained through the theoretical simulation and experimental test. The results can provide theoretical reference for design, debugging, maintenance and fault diagnosis of DRDNFV.

1 Structure and working principles of DRDNFV

The structure of the DRDNFV is shown in Fig. 1. When the command signal is input, the torque motor generates electromagnetic torque to make the armature flapper assemblies deflect around the center of the spring tube. Due to the hydraulic bridge principle[9], the control cavities on the both sides of the valve produce differential pressure to drive the spool to move. The LVDT at the right end will feed back the spool displacement signal to the torque motor to form the closed-loop control.

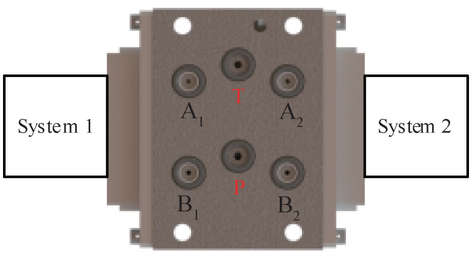

Fig. 1 Bottom of DRDNFV

The DRDNFV includes two sets of independent systems. Therefore, when one system fails, the other can still continue to feedback and control the main spool to make the valve work normally.

2 AMESim model of DRDNFV

2.1 Torque motor modeling

Ignoring the leakage flux, magnetic materials and the reluctance of non-working air gaps, the permanent magnet torque motor can be simplified as shown in Fig. 2[10-11].

According to Fig. 2, in the initial state, the magnetic fluxes in four air gaps are equal, the combined torque is zero, so the armature does not deflect. When there is the signal input, the combined torque is not equal to zero to make the armature and spring tube deflect.

To sum up, the simulation model of torque motor is built in AMESim, including coils, permanent magnets, magnetic assemblies and air gaps[12-13], as shown in Fig. 3.

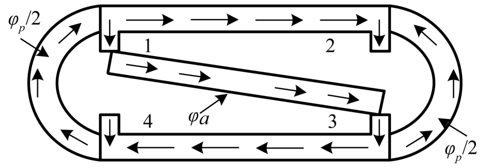

Fig. 2 Working principle of torque motor

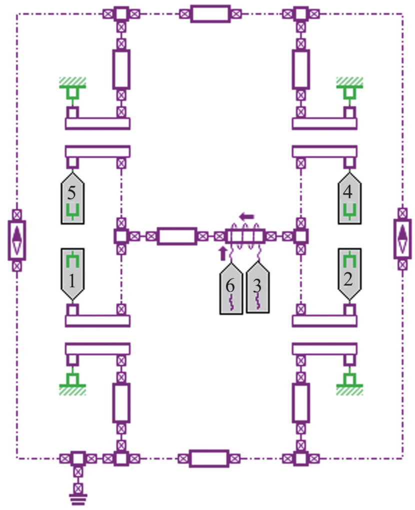

(a) AMESim model

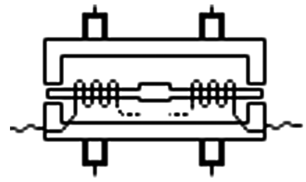

(b) Encapsulation model

Fig. 3 Model of moving-iron type torque motor

2.2 Armature assembly modeling

Because of the special structure of the armature assembly and the cancel of the feedback spring rod, there is no corresponding model in AMESim. It's necessary to build the six-port armature assembly model (Fig. 4).

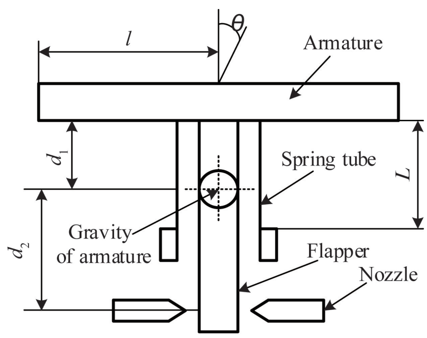

Fig. 4 Nozzle flapper assembly

(1) Deflection equation of armature

The armature motion includes two degrees of frecdem (DOF) of horizontal displacement x_g and deflection angle θ. During deflecting, the spring tube deforms[14], resulting in horizontal movement x_t. Therefore, the torque τ_{tube} and spring tube force F_{tube} can be written in the form of matrix.

$$\begin{vmatrix} F_{\text{tube}} \\ \tau_{\text{tube}} \end{vmatrix} = EI \begin{vmatrix} 12/L^3 & -6/L^3 \\ -6/L^3 & 4/L \end{vmatrix} \begin{vmatrix} x_t \\ \theta \end{vmatrix} = EI \begin{vmatrix} K_{11}x_g + (K_{11}d_1 + K_{12})\theta \\ K_{21}x_g + (K_{21}d_1 + K_{22})\theta \end{vmatrix} \tag{1}$$

where E——Young modulus of spring tube, MPa;
I—— Inertia moment of spring tube, kg · m^2;
L——Length of spring tube, mm;
d_1——Distance between armature center and bottom of spring tube, mm;
d_2—— Distance between armature center and nozzle, mm;
K_{11}——$12/L^3$, mm^{-3};
K_{12}, K_{21}—— $-6/L^2$, mm^{-2};
K_{22}——$4/L$, mm^{-1}.

(2) Hydrodynamic force equations of flapper

The hydrodynamic force of the left and right nozzles applied to the flapper is shown as

$$F_L = f_l - f_r \tag{2}$$

where F_L——Resultant hydraulic force on flapper, N;
f_l—— Hydraulic force on left flapper, N;
f_r—— Hydraulic force on right flapper, N.

(3) Equations of the armature motion

The equations of the armature motion are shown as

$$\begin{aligned} J\ddot{\theta} &= T_d - b_r\dot{\theta} - \tau_{\text{tube}} + F_L d_2 \\ &= T_d - b_r\dot{\theta} - EI(K_{21}x_g + (K_{21}d_1 + K_{22})\theta) \\ &\quad + (f_l - f_r)d_2 \end{aligned} \tag{3}$$

$$\begin{aligned} m\ddot{x}_g &= -b_t\dot{x}_g - F_{\text{tube}} + F_L \\ &= -b_t\dot{x}_g - EI(K_{11}x_g + (K_{11}d_1 + K_{12})\theta) \\ &\quad + (f_l - f_r) \end{aligned} \tag{4}$$

The state equation of the armature is expressed by the matrix as

$$\begin{vmatrix} \dot{\omega} \\ \dot{v}_g \\ \dot{\theta} \\ \dot{x}_g \end{vmatrix} = \begin{vmatrix} \dfrac{-b_r}{J} & 0 & \dfrac{-K_{22} - d_1K_{12}}{J} & \dfrac{-K_{12}}{J} \\ 0 & \dfrac{-b_t}{m} & \dfrac{-K_{12} - d_1K_{11}}{m} & \dfrac{-K_{11}}{m} \\ 1 & 0 & 0 & 0 \\ 0 & 1 & 0 & 0 \end{vmatrix} \begin{vmatrix} \omega \\ v_g \\ \theta \\ x_g \end{vmatrix} + \begin{vmatrix} T_d + (f_r - f_l)d_2 \\ f_l - f_r \\ 0 \\ 0 \end{vmatrix} \tag{5}$$

(4) AMEsim model of armature

First, the six-port armature is created and three external variables are added at each port. Second, internal variables and real parameters are set in the Type bar. Finally, C code is compiled to obtain the armature model, as shown in Fig. 5.

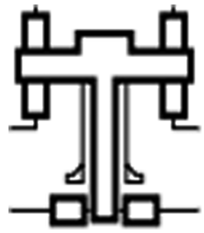

Fig. 5 Armature model

2.3 Nozzle assembly modeling

According to the armature's working principle, the nozzle assembly simulation model is built in AMESim, including the zero-velocity source sub-model, the spring damping sub-model and the flapper nozzle valve sub-model, as shown in Fig. 6.

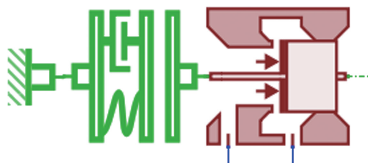

Fig. 6 Nozzle assembly model

2.4 AMESim overall simulation model

Based on the models of torque motor, armature and nozzle, by adding the throttle hole, variable volume cavity, fuel tank and other assemblies, the AMESim simulation model of DRDNFV is established, as shown in Fig. 7.

3 AMESim result analysis

3.1 Static characteristic curves in normal mode

The supplying pressure is set as 11.5 MPa. The frequenly of the input signal of torque motor is set as 0.02 Hz, the amplitude is set as 14 mA and the simulation duration is set as 200 s. The pressure and flow characteristics curves can be obtained as shown in Figs 8 – 9.

According to Figs 8 – 9, the pressure gain of the valve is 6.106 bar · mA, and the flow gain is 0.011 L · min · mA.

3.2 Static characteristic curves in double side clogged mode

The clogged phenomenon could be simulated by changing the equivalent diameter of the orifices[15]. Assuming that the clogged degree of the fixed orifices on double side is 0%, 20%, 30% and 40% in turn, the pressure and flow characteristics curves are obtained by simulation as shown in Figs 10 – 11.

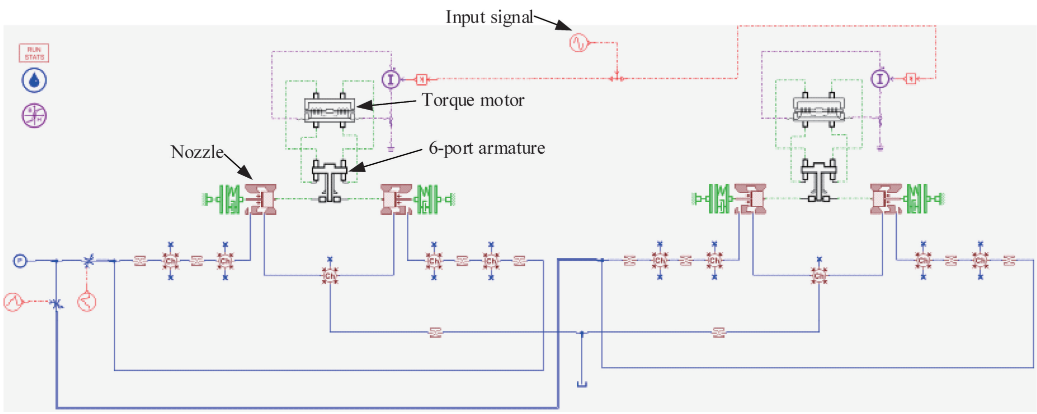

Fig. 7 DRDNFV simulation model

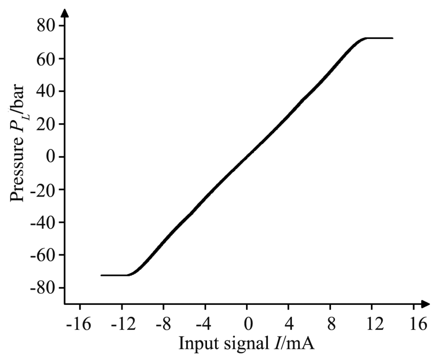

Fig. 8 Pressure characteristic curve

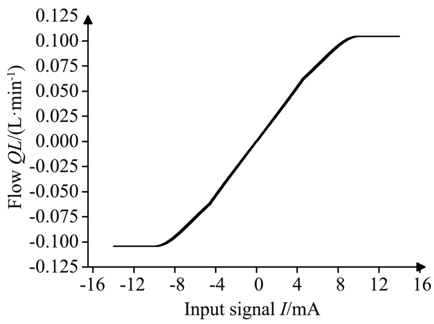

Fig. 9 Flow characteristic curve

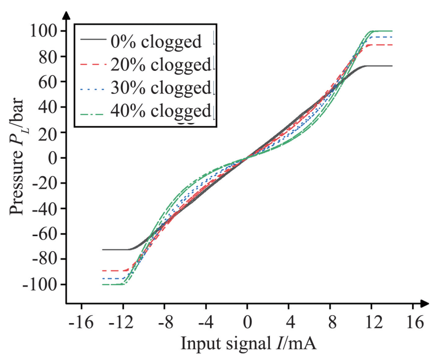

Fig. 10 Pressure characteristic curve in double side clogged mode

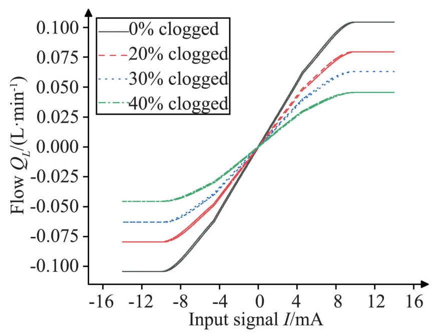

Fig. 11 Flow characteristic curve in double side clogged mode

According to Figs 10 – 11, the more seriously the fixed orifices on both sides are clogged, the stronger the throttling effect is, resulting in a larger pressure gain and smaller flow gain of the valve.

3.3 Static characteristic curves in right side clogged mode

Assuming that the clogged degree of the right fixed orifice is 0%, 20%, 30% and 40% in turn, the pressure characteristic curve can be obtained by simulation as shown in Fig. 12.

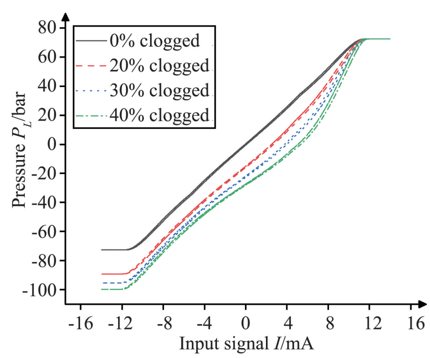

Fig. 12 Pressure characteristic curve in right side clogged mode

According to Fig. 12, when the right fixed orifice is clogged to different degrees, the zero bias reflected in the pressure characteristic curve also changes. The more serious the right orifice is clogged, the greater the zero bias is.

4 Experimental test

As shown in Fig. 13, on the test bench of DRDNFV, the pressure and flow characteristics test experiments are carried out and the curves are obtained as shown in Figs 14 – 15.

Comparing Fig. 8 and Fig. 14, it can be seen that the simulation results of the pressure characteristic curves are basically consistent with the experimental results. The pressure gain error is 10.5%, and it is in the allowable range of the project. Similarly, comparing Fig. 9 and Fig. 15, the error of flow gain is 10.8%, and it is in the allowable range of the project. The correctness of the AMESim simulation model is verified.

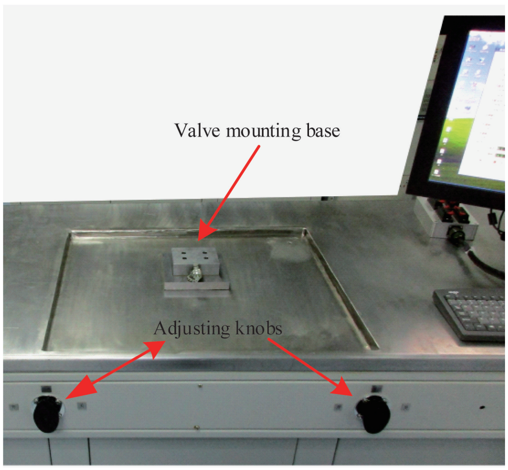

Fig. 13 Test bench of DRDNFV

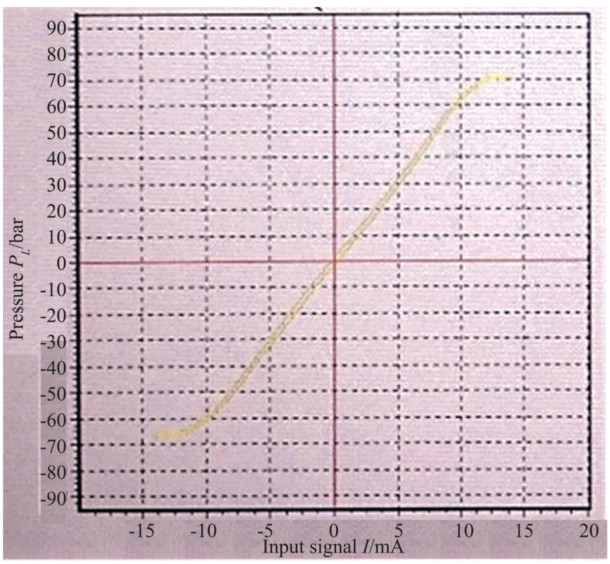

Fig. 14 Pressure characteristic curve

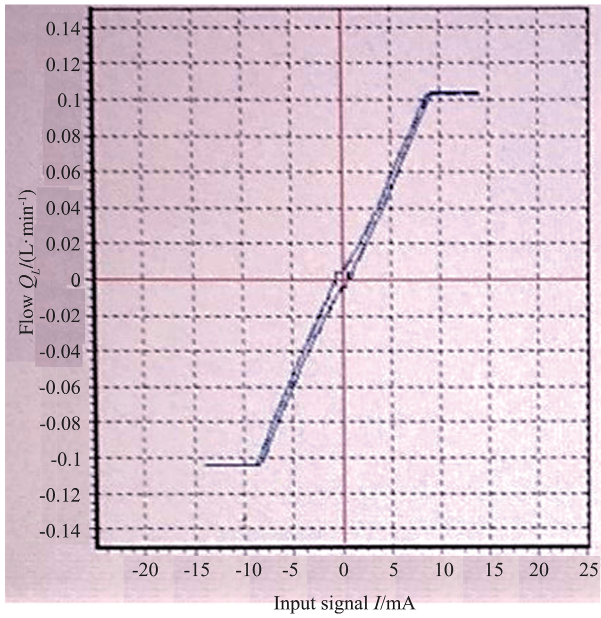

Fig. 15 Flow characteristic curve

5 Conclusions

(1) The static characteristic curves are plotted on the test bench. The trend of the experimental curves is basically consistent with the simulation results, which effectively verified the correctness of the theoretical analysis and simulation model.

(2) The effects of the clogged degree of fixed orifices on static characteristic of DRDNFV are simulated. The pressure gain becomes larger and the flow gain becomes smaller as the clogged degree increases.

(3) The AMESim simulation model of DRDNFV is built to lay the foundation for later performance analysis, fault simulation and fault diagnosis.

References

[1] FANG Q, HUANG Z. Developing process, research actuality and trend of electrohydraulic servo valve [J]. Machine Tool and Hydraulics, 2007, 35(11): 162-165. (In Chinese)

[2] CHEN Z G, DING F, CAI Y H. Research on characteristics of single-stage twin flapper-nozzle electrohydraulic servo valve [J]. Machine Tool and Hydraulics, 2007, 35(4): 114-116, 135. (In Chinese)

[3] CHEN C. Research on pressure characteristics of single-stage nozzle baffle electro-hydraulic servo valve [J]. Internal Combustion Engine and Parts, 2022, (4): 77-81. (In Chinese)

[4] WANG X Q, WANG W F. Modeling and simulation of ar-

mature assembly of double-stage dual-nozzle-flapper electro-hydraulic servo valve [J]. Machine Tool and Hydraulics, 2014, 42(23): 161-165, 199. (In Chinese)
[5] LI Y S. Physical model of two-stage nozzle-flapper electro-hydraulic servo-valve with force feedback [J]. Chinese Hydraulics and Pneumatics, 2021, 45(4): 69-73. (In Chinese)
[6] GORDIC D, BABIC M, JOVICIC N. Modelling of spool position feedback servo valves [J]. International Journal of Fluid Power, 2014, 5(1): 37-50.
[7] SHI S M. The fault diagnosis of the electro-hydraulic servo valve based on neural network [D]. Qinhuangdao: Yanshan University, 2022. (In Chinese)
[8] MU D J. Study on coupled vibration characteristics of electro-hydraulic servo valve and vibration control [D]. Beijing: Beijing Jiaotong University, 2015. (In Chinese)
[9] NIE S L, KONG X C, JIA G T. Orthogonal design and analysis of hydraulic bridge for water servo valve [J]. Journal of Mechanical Engineering, 2009, 45(6): 67-72. (In Chinese)
[10] QIN J Y, LI C C, YAN H. Effect of temperature on torque motor air gap reluctance and permanent magnet polarization magnetomotive force [J]. Machine Tool and Hydraulics, 2017, 45(9): 105-109. (In Chinese)
[11] YIN Y B, GUO W K, LI R H. Magnetic circuit modeling and characteristic analysis of torque motor considering magnetic leakage [J]. Journal of Harbin Engineering University, 2020, 41(12): 1840-1846. (In Chinese)
[12] LI L F, YU M H, MA C F, et al. Simulation and fault research for two stage double nozzle flapper electro-hydraulic servo valve based on AMESim [J]. Machine Tool and Hydraulics, 2017, 45(1): 177-180. (In Chinese)
[13] HUANG C C, YAN C K, ZHANG J N, et al. Analysis of influencing factors of servo torque motor output torque [J]. Chinese Hydraulics and Pneumatics, 2021, 45(7): 65-70. (In Chinese)
[14] WANG X L, JIANG J L, XIAN Y P, et al. Application and comprehensive performance test on the armature assembly of servo valve [J]. Flight Control and Detection, 2022, 5(1): 23-29. (In Chinese)
[15] ZHENG W M, LIU Y, ZHANG H L. Analysis of common fault of three-stage electro hydraulic servo valve [J]. Hydraulics Pneumatics and Seals, 2021, 41(11): 85-87. (In Chinese)

SUN Yanan, born in 1986. He is currently an engineer at Shijiazhuang Haishan Industrial Development Co. Ltd. He received his B. S. degree in 2011 from Hebei Normal University of Science and Technology, and M. S. degree in 2014 from Hebei University of Technology. His main research interest is in the repair technology of electro-hydraulic servo valve products.